Chromosoma (2025) 134:2
https://doi.org/10.1007/s00412-025-00828-2

RESEARCH

Towards identification of a holocentromere marker in the lepidopteran model *Spodoptera frugiperda*

Sylvie Gimenez[1] · Magali Eychenne[1] · Fabrice Legeai[2,3] · Sally Gamble[1] · Emmanuelle d'Alençon[1]

Received: 24 January 2025 / Revised: 27 January 2025 / Accepted: 12 February 2025

Abstract
Some insects have holocentric chromosomes, with multiple kinetochores rather than a single centromere. They also lack the CENP-A and CENP-C proteins, suggesting a kinetochore assembly process different from that of monocentric chromosomes. The homolog of CENP-T was recently shown to bind silent chromatin and to play a key role in kinetochore assembly in *Bombyx mori*, but its role in other insects with holocentric chromosomes is unknown. We identified kinetochore genes and analyzed their expression in *Spodoptera frugiperda*. We silenced the kinetochore genes *cenp*-L, *cenp*-S, *cenp*-X and *ndc*80 and searched for chromosome segregation defects in *Sf*9 cells. All kinetochore genes except *cenp*-S were more strongly expressed in gonadal than in somatic tissues. Immunofluorescence microscopy and RT-qPCR demonstrated the effective silencing of the target genes by transfection with dsRNA. In Sf9 cells depleted of CENP-L and NDC80, immunofluorescence microscopy revealed increases in mitotic index and in the proportion of cells with unaligned chromosomes or multipolar spindles. The depletion of CENP-S and CENP-X had no effect on mitotic index and no division defects were observed. This suggests that CENP-L and NDC80 play key roles in chromosome segregation, whereas the functions of CENP-S and CENP-X remain unknown. We have begun to characterize the kinetochore proteins (CENP-L, CENP-S, CENP-X, NDC80), a prerequisite for holocentromere identification in *S. frugiperda*. This study also provides the first information about the role, in Lepidoptera, of CENP-L, a protein essential to the structure of the constitutive centromere-associated network in species with monocentric chromosomes.

Keywords Kinetochore · Holocentric chromosome · Centromere · RNAi · Chromosome segregation · Lepidoptera

Introduction

Species with holocentric chromosomes have emerged at least 14 times during evolution, in both the plant and animal kingdoms (Melters et al. 2012). The distribution of centromere activity along the length of the chromosome has several functional consequences (see (Mandrioli and Manicardi 2020) for review), including a greater resistance to breakage, particularly after X-ray irradiation (Zedek and Bures 2018), more rapid rearrangements than in species with monocentric chromosomes (Coghlan and Wolfe 2002; d'Alencon et al. 2010), and a need for meiotic adaptation to overcome the deleterious effects of the opposing forces exerted on chiasmata in metaphase I (Melters et al. 2012). This adaptation may occur through a restriction of kinetochore activity to the telomeres as in *C. elegans* (Dumont et al. 2010; Howe et al. 2001; Monen et al. 2005), or through inverted meiosis as in some lepidopterans (Lukhtanov et al. 2018), although the frequency of inverted meiosis in this group is unknown.

The best characterized model of holocentric chromosomes is that of the nematode *C. elegans* (Buchwitz et al. 1999). Holocentric chromosomes also occur in at least four orders of insects (Melters et al. 2012). The holocentric chromosomes of these insects have been reported to lack the histone-like protein CENP-A (Cortes-Silva et al. 2020), which is considered to be a ubiquitous marker of the centromere in eukaryotes other than early diverging fungi and kinetoplastids (Ishii and Akiyoshi 2022). However, the available genomic data indicate that CENP-A is present in some hemipterans with holocentric chromosomes but absent

✉ Emmanuelle d'Alençon
emmanuelle.d-alencon@inrae.fr

[1] DGIMI, Univ Montpellier, INRAE, Montpellier, France

[2] BIPAA, IGEPP, INRAE, Institut Agro, University of Rennes, Rennes, France

[3] University of Rennes, INRIA, CNRS, IRISA, Rennes, France

Published online: 11 March 2025

from others (Cortes-Silva et al. 2020). Given the key role of CENP-A in kinetochore assembly in species with monocentric chromosomes, insects lacking this protein must have an alternative pathway for kinetochore assembly. This pathway probably involves other kinetochore proteins, and further studies are required to determine the role and hierarchy of these proteins in the kinetochore assembly process in species with holocentric chromosomes devoid of CENP-A. Many studies have focused on the kinetochore proteins of species with monocentric chromosomes, but there have been only three recent functional studies of kinetochore genes in cell lines from a single insect species with holocentric chromosomes: the silkworm *Bombyx mori*, a lepidopteran (Cortes-Silva et al. 2020; Mon et al. 2017; Senaratne et al. 2021). Mon et al. (2017) identified the outer kinetochore proteins NDC80, spc24 & 25, Mis12, Dsn1 and Nnf1 through bioinformatics and RNAi screening in BmN4-sid1 cells (Mon et al. 2017). The silencing of these genes leads to G2/M cell cycle arrest and an increase in cellular DNA content, as shown by flow cytometry (Mon et al. 2017). Immunofluorescence microscopy showed that these proteins were associated with chromosomes and located on either side of the metaphase chromosomes. In addition, Cortes-Silva et al. (2020) identified and characterized the inner kinetochore proteins CENP-M, N, I and CENP-T by RNAi and microscopy on BmN4-sid1 cells (Cortes-Silva et al. 2020). Senaratne et al. (2021) showed, by ChIP-seq, that the inner kinetochore protein CENP-T colocalizes with the histone marker H3K27me3 in unsynchronized *B. mori* cell populations, suggesting that the centromere is excluded from active chromatin (Senaratne et al. 2021). The centromere of the silkworm has not yet been characterized during mitosis *in vivo*. A localized centromere has been described in meiosis but not in mitosis (Holm and Rasmussen 1980; Rosin et al. 2021). However, little is known about the molecular determinism of chromosome segregation during meiosis in *Bombyx mori* and other lepidopterans, with the exception of the presence of CENP-T, absence of CENP-A and the fact that kinetochore assembles at non-telomeric loci (Hockens et al. 2024; Rosin et al. 2021) in these species.

Spodoptera frugiperda, also known as the fall armyworm (FAW), is another lepidopteran (Noctuidae) with holocentric chromosomes (Gerbal et al. 2000), in which we have annotated kinetochore gene homologs in the published reference genome (Gouin et al. 2017). Some of the genes missing from this annotation have been identified by immunoprecipitation and mass spectrometry (IP-MS) in cell lines stably expressing Flag-tagged kinetochore components (Cortes-Silva et al. 2020). The outer kinetochore of *Spodoptera frugiperda* is composed of Ndc80, Nuf2, Spc24, Spc25, Dsn1, Mis12, Nsl1, Nnf1 and Kln1. The inner kinetochore consists of CENP-L, CENP-N, CENP-I, CENP-K, CENP-M and CENP-T. Not only are CENP-A and CENP-C absent, but several other inner kinetochore proteins, such as CENP-O, CENP-P, CENP-Q, CENP-U, CENP-R, CENP-S, CENP-X, were also missing in the IP-MS analysis. Homology-based analyses identified putative genes for only two of these proteins, *cenp-S* and *cenp-X* (Gouin et al. 2017), but we cannot rule out the possibility that distant homologs of these proteins are present in Lepidoptera. Using an ovary cell line (*Sf*9) EST library, we have characterized a CENP-*B* homolog with the features of a domesticated transposase resembling the CENP-B protein of humans (d'Alençon et al. 2011).

In this study, we identified kinetochore genes and explored their patterns of expression in the gonadal and non-gonadal tissues of *Spodoptera frugiperda*.

For detailed functional studies of centromeric genes, it was essential to develop an efficient but mild protocol for transfecting cell lines with RNAi to enable us to detect a phenotype of mis-segregation. The method needed to be "mild", to prevent interference with cell division, which occurs in a small proportion of cells at any given time (about 5% (d'Alencon et al. 2011) in cultured cells, which grow asynchronously). It needed to be efficient to ensure that these dividing cells were efficiently depleted of the target mRNA. Our first attempts based on protocols developed in a previous study (Agrawal et al. 2004) did not achieve these objectives (d'Alencon et al. 2011). As we aimed to study chromosome segregation, we wished to avoid soaking in a solution of the exogenous *C. elegans* SID protein (CeSid) and the use of cell lines producing this protein constitutively (Chen et al. 2021; Xu et al. 2013) for membrane permeabilization. Transfection with dsRNA in the presence of Cellfectin II is an effective means of silencing luciferase or IAP genes (Gurusamy et al. 2020) in lepidopteran cells, but this method results in changes to cell morphology even at low concentrations, whereas no such changes are observed with Fugene HD (Gurusamy et al. 2020). We therefore used Fugene HD as the transfecting agent. This polycation lipid mixture is known to have little or no cytotoxicity to animal cells (Jacobsen et al. 2004). We aimed to establish transfection conditions in which at least 90% of the target kinetochore mRNAs were depleted.

We then transfected *Sf*9 cells with dsRNA precursors to silence one of the outer kinetochore genes encoding NDC80, a protein for which depletion has been shown to lead to aneuploidy in *Bombyx mori* cells (Mon et al. 2017), as a positive control, and three putative inner kinetochore genes (encoding CENP-L, CENP-S, and CENP-X). In *Bombyx mori* and other organisms, the depletion of kinetochore components results in mitotic defects (Baudoin and Cimini 2018; Cortes-Silva et al. 2020; Maiato et al. 2003). We performed immunofluorescence (IF) microscopy analyses on the transfected cells. As the three previous studies were all performed in *Bombyx mori* (Cortes-Silva et al. 2020; Mon et al. 2017; Senaratne et al. 2021), we decided to study

another lepidopteran species with holocentric chromosomes (*Spodoptera frugiperda*).

Materials and methods

Cell lines, moths and genes targeted

The *Sf*9 cell line was obtained from ATCC. The pJGFPH plasmid (Bossin et al. 2003) carries the *gfp* template for dsRNA synthesis. *S. frugiperda* (Guadeloupe isolate, corn strain) was reared at 25 °C on a synthetic medium developed in a previous study (Poitout and Bues 1974).

The target genes for dsRNA (Gene ID from OGS2.2 (Gouin et al. 2017)) are listed in Table 1, together with the primers used for template amplification, insertion of the T7 promoter by PCR and quantification of expression by RT-qPCR.

dsRNA synthesis

Total RNA was extracted from FAW larvae (L6 instar) with the EZNA Total RNA Kit (OMEGA Bio-tek) and reverse-transcribed with the Superscript II reverse transcriptase (INVITROGEN). This cDNA was used as a template for PCR amplification with the following primer pairs: pX5'-pX3' for CENP-X, pS5'-pS3' for CENP-S, pN5'-pN3' for CENP-N, pL5'-pL3' for CENP-L. The PCR fragments obtained were used as a template for a second round of PCR with the following primer pairs to introduce the T7 promoter sequence: pXT75'-pXT73' for CENP-X, pST75'-pST73' for CENP-S, pNT75'-pNT73' for CENP-N, pLT75'-pLT73' for CENP-L. As a control dsRNA, a 692 bp fragment of GFP DNA was amplified by PCR amplified from pJGFPH (Bossin et al. 2003) and inserted between the two convergent T7 promoters in the L4440 plasmid, a gift from Andrew Fire (Addgene plasmid # 1654; http://n2t.net/addgene:1654; RRID:Addgene_1654). The PCR fragments were purified by ethanol precipitation and their sequences were checked by Sanger sequencing. *In vitro* transcription was performed with the T7 RiboMAX Express RNAi System (Promega).

dsRNA silencing (transfection)

We used a previously described protocol (Gurusamy et al. 2020) with a modification of the ratio of dsRNA to Fugene HD and a change in the transfection medium. We incubated 2 µg of dsRNA with 200 µl TC100 medium (GIBCO) supplemented with 2% serum in the presence of Fugene HD transfection reagent (Promega, added at a ratio of 1:8 v/v) for 15 min before transfection. *Sf*9 cells at 30% confluence were transfected with 50 µl of this mixture (500 ng dsRNA per well, in 12-well plates). We assessed the efficiency of dsRNA silencing by extracting total RNA from the transfected cells one and five days after transfection, as previously described. The relative amounts of mRNA for the targeted genes after cell transfection were determined by RT-qPCR with the following primer pairs: pXF-pXR for *cenp*-X, pSF-pSR for *cenp*-S, pNF-pNR for *Ndc*80, pLF-pLR for *cenp*-L, ELF1-F, ELF1-R for *Elf1*α. The results obtained were compared with those for a control gene, *Rpl*32, amplified with the rpl32-F and rpl32-R primers (see cell lines and genes targeted). Normalization was performed with respect to control cells transfected with a dsRNA against GFP.

IF microscopy (antibodies, IF labeling, observation, cell counts)

For the visualization of chromosome segregation defects, *Sf*9 cells were grown on glass coverslips in cell culture plates containing TC100 medium supplemented with fetal bovine serum 5%. The coverslips were rinsed once in 1 × PBS and fixed. α-tubulin was then localized on the fixed cells in PBS with 4% paraformaldehyde (Thermoscientific) as previously described (Li et al. 1996) except that a 15-min blocking step in IF buffer containing 1% BSA at room temperature was added after the permeabilization of the cells and nuclei in 3% Triton X-100. Mouse anti-α-tubulin (Monoclonal Anti-α-Tubulin antibody produced in mouse, ref T9026, Merck) antibodies were used at a dilution of 1:4000, and were detected with Alexa Fluor 568 (Invitrogen)-conjugated anti-mouse secondary antibodies used at a dilution of 1:1000. Dividing cells were detected by incubation with a rabbit monoclonal antibody against phosphorylated histone H3 S10 (clone 63-1C-8, ZooMAb® Rabbit Monoclonal antibody, Merck) at a dilution of 1:100 followed by an Alexa Fluor 568 (Invitrogen)-conjugated anti-rabbit secondary antibody. Chromosomes were stained by incubation with Hoechst stain at a dilution of 1:10,000 in 1 × PBS for 5 min at room temperature in the dark. The cells were mounted in fluorescence mounting medium (Dako) and observed under a microscope (Leica Thunder). Cells were counted with Image J software for determination of the mitotic index.

RNA extraction, library preparation, Illumina sequencing, read mapping and counts

We present here RNA-Seq data obtained from the gonads of the insect. For the fat-body data, we reused the RNA-Seq data reported in a previous study (Robin et al. 2023). However, both sets of RNA-Seq data were obtained in the same way, in parallel, as follows. The gonads and fat bodies of fifth-instar larvae were dissected out, washed in PBS and transferred directly to the TRK lysis buffer from EZNA Total RNA kit I (Omega) for total RNA extraction. Samples were stored at −80 °C until use. Total RNA was extracted

Table 1 Gene targets for dsRNA silencing and primers

Gene template for/Gene ID in OGS2.2 (Gouin et al. 2017)	Primer name	DNA sequence
CENP-L GSSPFG00023246001.3-PA	pL5'	ATCGATCAGAGCCTGCTTGG
	pL3'	TTGTTCACCTCGTTCCAGCA
	pLT75'	GGATCCTAATACGACTCACTATAGGATCGATCAGAGCCTGCTTGG
	pLT73'	GGATCCTAATACGACTCACTATAGGTTGTTCACCTCGTTCCAGCA
	pLF	AGTGACTCATCTCGCAGCAC
	pLR	TCTGGATGTCCCCAACTTCA
	pL5'bis	ATGGCTATGTATCGATCAGAGCCTGCTTGG
	pL3'bis	TGAATCAGATGCAGATGCATTGCCGGAATC
	pNtgfpL5'	GGGGACAAGTTTGTACAAA AAAGCAGGCTTCATGGCTATGT ATCGATCAGAG
	pNtgfpL3'	GGGGACCACTTTGTACAAGAAAGCTGGGTCCTA TGAATCAGATGCAGATGCATTG
CENP-S GSSPFG00001415001.3-PA	pS5'	CTATTGGCTCGGAAACTTGC
	pS3'	TCGAAGTTCGCTGTTTCATTC
	pST75'	GGATCCTAATACGACTCACTATAGGCTATTGGCTCGGAAACTTGC
	pST73'	GGATCCTAATACGACTCACTATAGGTCGAAGTTCGCTGTTTCATTC
	pSF	TCATTCAGTTGCTTTAACTTTCCTC
	pSR	GTACATCCCGGTGCAAAGC
	attB1FdS	AAAAAAGCAGGCTTCGAAGGAGATAGAACCATGTCGTCTT TTGAAAATCTATCGTC
	attB2rvS	AGAAAGCTGGGTCATCAAACGTTAAATCAATCATATTATC
	attB1adaptS	GGGGACAAGTTTGTACAAA AAAGCAGGCT
	attB2adaptS	GGGGACGACTTTGTACAAGAAAGCTGGGT
CENP-X GSSPFG00011580001.1-PA	pX5'	CAACGAGAACGATGAGGACA
	pX3'	GTAGGAATGGGCAGAAGCTG
	pXT75'	GGATCCTAATACGACTCACTATAGGCAACGAGAACGATGAGGACA
	pXT73'	GGATCCTAATACGACTCACTATAGGGTAGGAATGGGCAGAAGCTG
	pXF	GCTTCATGCGTCATATAAAGACTATA
	pXR	TGCTTTCATCAATTATTAACAACCAAA
	pNtgfpX5'	GGGGACAAGTTTGTACAAAAAAGCAGGCTTC ATGGCTCGTAATAGCAACGAG
	pNtgfpX3'	GGGGACCACTTTGTACAAGAAAGCTGGGTCCTA AGGGAAATCCAGCATCAGCTG
NDC80 GSSPFG00005966001.4-RA	pN5'	TGTGGCAGAAGAAGACGTTG
	pN3'	GCAGCTTGAGTTCCTCCATC
	pNT75'	GGATCCTAATACGACTCACTATAGGTGTGGCAGAAGAAGACGTTG
	pNT73'	GGATCCTAATACGACTCACTATAGG GCAGCTTGAGTTCCTCCATC
	pNF	CAGTCCACGCTCAAAACTGA
	pNR	GGACTCCAACTCCTGCTTCA
RPL32	rpl32-F	TACAATCGTCAAAAAGAGGACGA
	rpl32-R	AAACCATTGGGTAGCATGTGA
ELF1-F	ELF1-F	GGACACGTCGACTCCGGCAAG
	ELF1-R	CTCCGTGCCAGCCAGAAATGG

with EZNA Total RNA kit I, according to the manufacturer's instructions (Omega). RNA samples were treated with the TURBO DNA-free kit (Ambion) to eliminate contaminating genomic DNA. RNA concentration and integrity were assessed with a NanoDrop ND-1000 spectrophotometer and an Agilent 2100 Bioanalyzer, respectively. Total RNA samples with an RNA integrity (RIN) score ≥ 9 were retained for RNA sequencing. For each replicate (three for the fat body, two for the gonads), total RNA was extracted from the fat bodies of 25–28 larvae and the testes of five larvae.

Library preparation and RNA sequencing were performed by the Montpellier GenomiX (MGX) sequencing facility (CNRS, Montpellier, France). Briefly, polyA mRNA was isolated with oligo(dT) beads and fragmented. The first cDNA strand was then synthesized with random primers and Superscript Reverse Transcriptase II (Invitrogen). The

second cDNA strand was synthesized. Two cDNA libraries were generated from the Illumina TruSeq Stranded mRNA sample and sequenced on an Illumina HiSeq 2500 platform to generate 125 bp paired-end reads. Libraries were validated with the Fragment Analyzer system and the Standard Sensitivity NGS kit.

Raw reads were aligned with the sfC.ver5.fa reference genome sequence for *Spodoptera frugiperda* (Nam et al. 2018) with STAR v20201, mode alignReads, and the options –outFilterMultimapNmax 5 –outFilterMismatchNmax 3 –alignIntronMin 10 –alignIntronMax 50000 –alignMatesGapMax 50000 –outSAMtype BAM SortedByCoordinate –outSAMstrandField intronMotif. We obtained a mean of 24 million cleaned reads per replicate. The counts per gene were obtained with OGS6.0, using featureCounts from subread v1.6.0, with the options -g gene_id -t exon -C -p -s 0 -M –fraction.

Analysis of differential gene expression

We assessed differences in gene expression between insect tissues (male gonads vs. fat body in fifth instar larvae), using the read count data as input for the R package DESeq2 (Anders and Huber 2010). DESeq2 uses negative binomial generalized linear models to test for differential expression. An adjusted *p*-value for multiple testing was computed with the Benjamini–Hochberg procedure to control for false discovery rate (FDR). Results with a FDR < 0.05 were considered statistically significant.

Meiotic chromosome spreads

Meiotic chromosomes were obtained from the gonads of male fifth-instar *S. frugiperda* larvae. The gonads were treated with 0.5% sodium citrate for 15 min then left in freshly prepared fixative (3:1 ratio of 60% acetic acid and methanol) for 15–30 min. The gonads were then cut into slices which were spread on the slide in 60% acetic acid, on a plate heated to 45 °C. The slides were stored at −20 °C and mounted in mounting medium (DAKO). The slides were observed using a microscope (LEICA THUNDER).

Cellular localization of CENP proteins

We used the Gateway-compatible vectors developed by (Maroniche et al. 2011) for live imaging in insect cells, to construct plasmids expressing CENP-L, CENP-S and CENP-X in fusion with green fluorescent protein (GFP).

For that, we generated attB-PCR products from cDNA of the larvae of *Spodoptera frugiperda* (L6 stage) using the primers pairs listed on Table 1 through either a single or two steps of amplification by PCR with iProof High-Fidelity DNA polymerase (Biorad) (First primers pair pL5'bis—pL3'bis then pNtgfpL5'- pNtgfpL3'for CENP-L, first primers pair attB1FdS—attB2rvS, then attB1adapt-Sand attB2adaptS for CENP-S and the only primers pair pNtgfpX5' and pNtgfpX3'for CENP-X). We then used the "one-tube" protocol for cloning attB-PCR products directly into the destination vectors pIB-GW for CENP-L and CENP-X (GFP in Nterm) or pIB-WG for CENP-S (GFP in Cterm, cf scheme on Supplementary Fig. 4 a) with the intermediate vector pDONR221 and the kit "PCR cloning system with gateway technology with pdonr221 omnimax2 competent cells" from Invitrogen plus the Gateway lr clonase ii enzyme mix from Invitrogen. The location of functional domains in the protein sequences guided the choice for Nt or Ct fusions. Ligations were used to transform omnimax competent cells on LB agar selecting for Ampicillin. Ampicillin resistant and Chloramphenicol sensible clones were screened by PCR with the primers used to obtain attB-PCR fragments to identify recombinant clones. Final candidate clones were amplified and plasmid extracted using Plasmid maxi kit from Qiagen, constructs were checked by Sanger sequencing. 0.5 to 1 µg of plamid DNA was used to transfect *Sf*9 cells with Fugene HD transfection reagent (Promega) on coverslips in 12 wells culture plates with TC100 medium. Live imaging was performed as described in (Maroniche et al. 2011) at 48 h and 72 h post-transfection using a 63 × objective using a microscope (LEICA THUNDER).

Results

Pattern of kinetochore gene expression in the gonadal and non-gonadal tissues of the insect

Several studies have shown that genes involved in the same biological process tend to be co-expressed at transcriptional level (Mon et al. 2022; Somma et al. 2008). One approach to characterizing kinetochore genes in this non-model organism is, therefore, to analyze the expression patterns of these genes in different tissues, checking for similarities and differences. We performed an RNA-Seq analysis comparing a tissue known to contain many meiotic and mitotic cells in *Bombyx mori* and *Spodoptera* (Rosin et al. 2021; Salama et al. 1971) (gonads of 5th instar male caterpillars) and a tissue with moderate levels of mitotic activity, the fat body, which grows through mitosis and endoreplication in larvae (Skowronek et al. 2021). A microscopy analysis of chromosome spreads of the male gonads of fifth-instar larvae confirmed that cells in meiotic prophase and some cells in mitosis were also present in the gonads of *Spodoptera frugiperda* (Supplementary Fig. 1). We obtained a mean of 23.9 million reads per replicate, about 18.6 million of which (78%) mapped to unique sites on reference genome version 5 of *Spodoptera frugiperda* (Supplementary Table 1, Mapping). The gene

expression profiles of the gonads and fat bodies were compared with DESeq2 software, which can be used to analyze differential gene expression between conditions based on read counts mapping to particular coding sequences (cpm, counts per million reads mapped on OGS6.0, and genes for which at least 10 reads in the two tissues were considered). The $\log_2$ fold-change for each gene was plotted as a function of mean expression — *i.e.* the mean number of counts normalized by size factors (Supplementary Fig. 2A). Blue dots correspond to genes displaying significant differential expression between the gonads and the fat body, at a FDR of less than 0.05. We also performed principal component analysis (PCA; Supplementary Fig. 2B) on the various samples (tissues, replicates). The variance between tissues was greater (95%) than that between replicates, which grouped together. Differential expression (at least a two-fold difference in expression levels) was detected for 6483 of 21,839 genes (29.69%), with a FDR < 5%. The DESeq2 tab of Supplementary Table summarizes the gene ID information for all the inner and outer kinetochore proteins of *Spodoptera frugiperda* studied (annotated in (Gouin et al. 2017) and identified by IP-mass spectrometry in (Cortes-Silva et al. 2020)), the results of DESeq2 and read counts (cpm). All the outer kinetochore genes studied were significantly overexpressed in the gonads relative to the fat body. Except *cenp-S*, the other inner kinetochore genes are also overexpressed in gonads versus fat body. Sixteen of the 17 kinetochore genes (94%) were found to be overexpressed in the testis relative to the fat body at a FDR < 5%. The heatmap in Fig. 1 shows a large cluster of genes with a low levels of expression in the fat body and much higher levels of expression in the testis, including *Ndc80, cenpT, cenpL.*

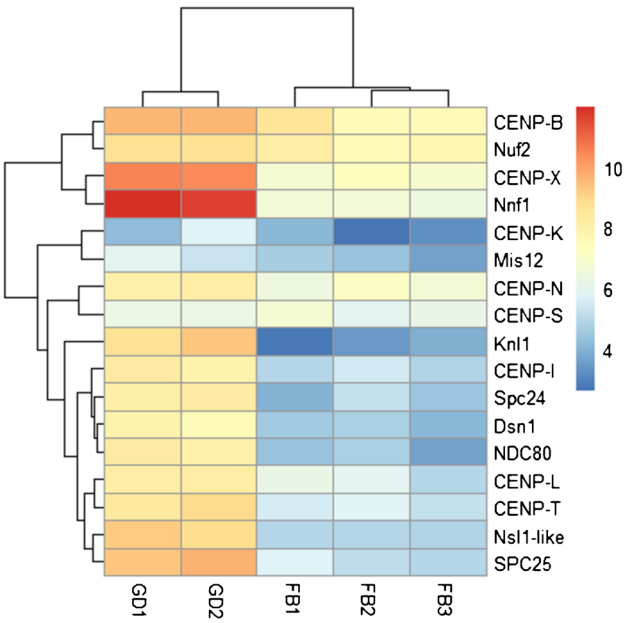

Fig. 1 Relative levels of expression in gonadal and non-gonadal tissues of inner kinetochore genes and the outer kinetochore gene *ndc80*. The heatmap shows the relative levels of expression of genes in the testis (GD for gonads) and the fat body (FB) for each gene, with Z-score normalization

A mild and efficient dsRNA silencing method for studying chromosome segregation

An RNA interference silencing protocol, with Fugene as the transfection agent, was applied to lepidopteran *Sf*9 cells (modified from (Gurusamy et al. 2020), see material and methods). We first assessed silencing efficiency visually by fluorescence microscopy with GFP. The cotransfection of *Sf*9 cells with a dsRNA against *gfp* and a plasmid carrying the *gfp* gene abolished the fluorescence obtained when cells were transfected with the plasmid only (Supplementary Fig. 3). Differential interference contrast (DIC) microscopy showed that treatment with Fugene HD–dsRNA complex mixtures had no detectable effect on cell morphology or proliferation, which remained similar to that in untransfected cells (Supplementary Fig. 3 B and 3C). We then targeted genes from the constitutive centromere-associated network (CCAN) — CENP-L, CENP-S, CENP-X — and NDC80, which is part of the NDC80 complex associated with the Kln1 and Mis12 complexes involved in the KMN network (Westhorpe and Straight 2013) (Fig. 2A and Table 1 for target gene IDs and primers). We performed two independent transfections with each dsRNA and extracted total RNA from the transfected cells one and five days after transfection. The level of kinetochore gene expression after silencing was calculated relative to the rpl32 housekeeping gene marker in RT-qPCR experiments, with normalization against control cells transfected with a dsRNA against GFP, the Ef1α gene serving as negative control. One or five days after transfection, residual *cenp*-L expression was 8.4% and 8.1% that of control cells, respectively. Residual expression levels were 8.0% and 11% of control levels, respectively, for *cenp*-S, 9.5% and 6.8% of control levels, respectively, for *cenp*-X, and 6.7% and 5.8% of control levels, respectively, for *Ndc*80 (Fig. 2B). We therefore concluded that dsRNA silencing was efficient in our conditions. Silencing efficiency was similar one and five days after transfection and we chose an intermediate time point, three days after transfection, for subsequent functional analysis.

Mitotic indices in cells with silenced kinetochore genes

The progress of the cell cycle is tightly regulated, particularly during mitosis, when the spindle assembly checkpoint (SAC) delays anaphase onset until all chromosomes are biorientated (for review (McAinsh and Kops 2023)). We

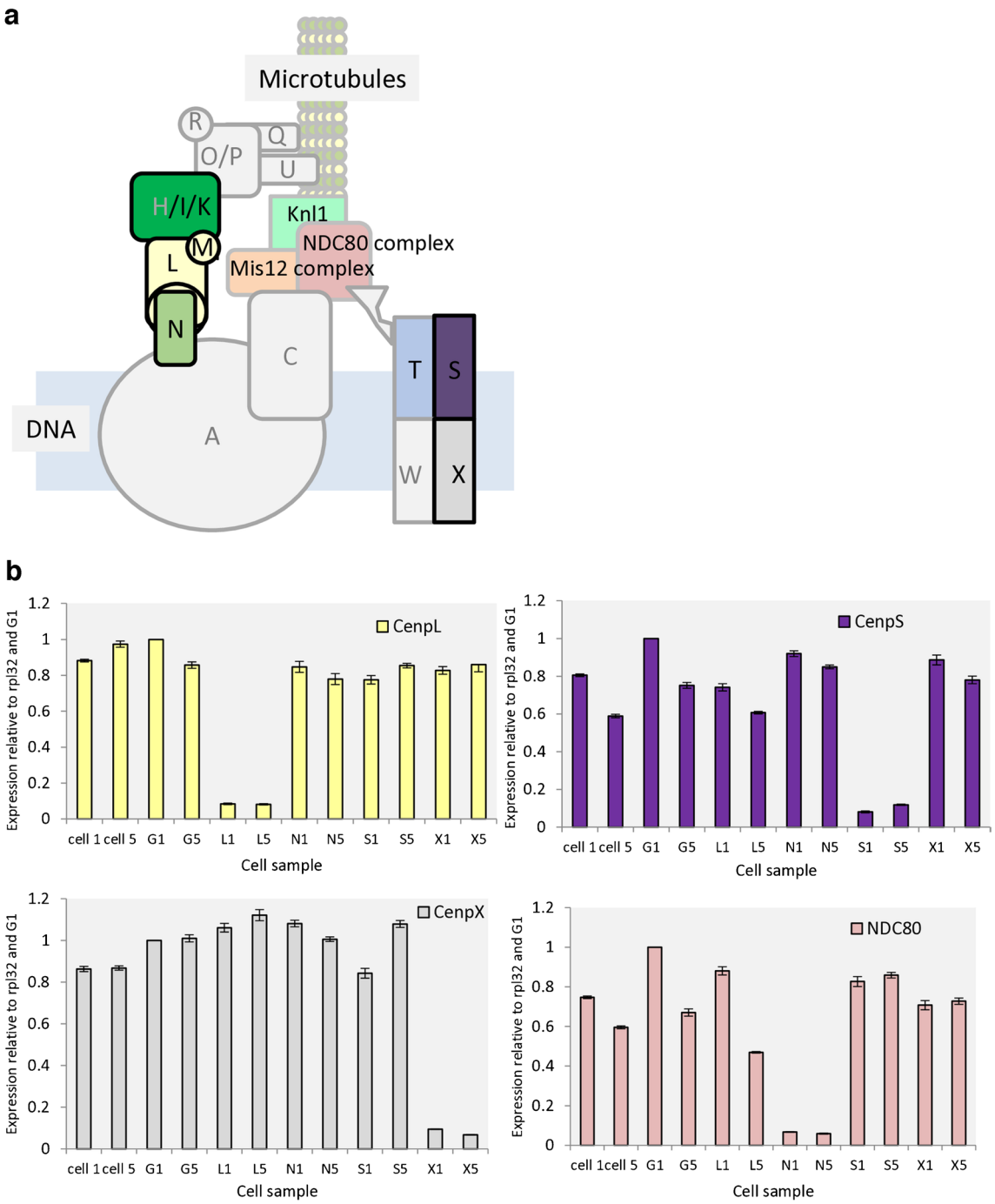

Fig. 2 Kinetochore genes silenced and silencing efficiency. **A**. The genes targeted by the dsRNAs cenp-L, S and X encode proteins of the constitutive centromere-associated network (CCAN). NDC80 is part of the KMN network, which includes the NDC80 complex (adapted from (Westhorpe and Straight 2013)). Gray boxes represent human kinetochore proteins for which no homolog was found in *S. frugiperda* and colored boxes represent kinetochore proteins or complexes for which genes have been annotated in the *Spodoptera frugiperda* genome (Cortes-Silva et al. 2020; Gouin et al. 2017). **B**. RT-qPCR analysis of the efficiency of silencing for the target genes *cenp*-L, *cenp*-S, *cenp*-X, *Ndc*80 after treatment with dsRNA for one or five days. Cell 1 and cell 5: Untransfected cells at 1 and 5 days, respectively. G1 and G5: Cells transfected with the dsRNA against GFP for 1 and 5 days, respectively. L1 and L5: Cells transfected with the dsRNA against CENP-L for 1 and 5 days, respectively. N1 and N5: Cells transfected with the dsRNA against NDC80 for 1 and 5 days, respectively. S1 and S5: Cells transfected with the dsRNA against CENP-S for 1 and 5 days, respectively. X1 and X5: Cells transfected with the dsRNA against CENP-X for 1 and 5 days, respectively

therefore hypothesized that the impairment of kinetochore gene expression would affect the proportion of the cells in M phase. We calculated mitotic indices for cells lacking CENP-L, CENP-S, CENP-X, or NDC80 and for control cells transfected with a dsRNA against *gfp* by immunofluorescence microscopy with antibodies against histone H3 phosphorylated on the serine in position 10, a marker of mitosis (Hendzel et al. 1997; Prigent and Dimitrov 2003). In *Sf*9 cells, this antibody labels cells in which the chromosomes are in (pro)metaphase or anaphase (Fig. 3A). In two independent transfection experiments, the mitotic index was 4% in control cells (Fig. 3B). It was not significantly different in cells in which *cenp*-S (4%) or *cenp*-X (3.8%) was silenced, whereas it doubled (7.2%) or tripled (12.0%) after the dsRNA-mediated silencing of *cenp*-L and *Ndc*80, respectively (Fig. 3B).

Segregation defects in cells with silenced kinetochore genes

Despite of the existence of highly effective mechanisms for correcting segregation errors in normal cells (reviewed in

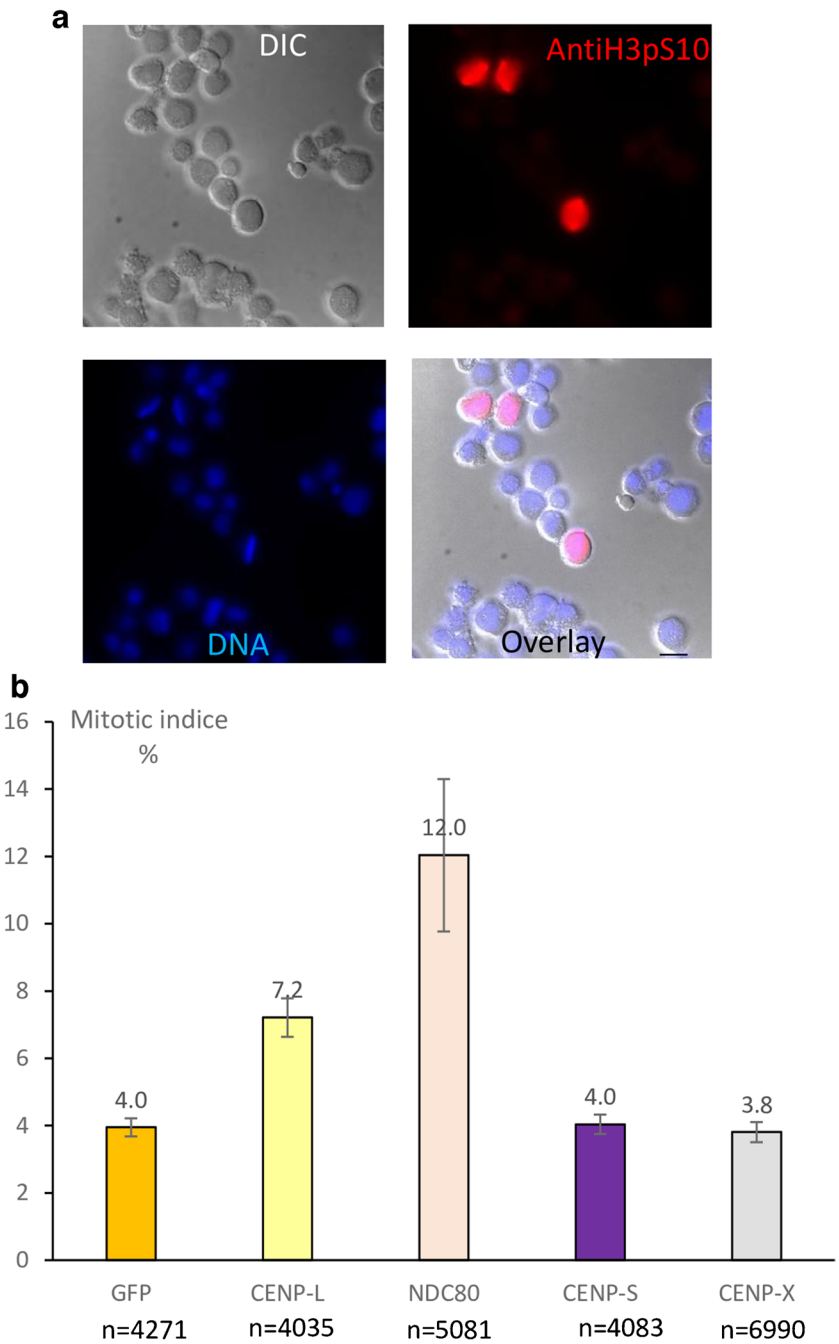

Fig. 3 Labeling of dividing cells and mitotic indices in *Sf*9 cells after transfection with the dsRNAs against *gfp* and centromeric genes. **A**. Dividing *Sf*9 cells were identified on immunofluorescence microscopy after labeling with antibodies against phosphorylated histone H3 S10 and detection with Alexa Fluor 568-conjugated anti-rabbit secondary antibodies. Top left) DIC (differential interference contrast). Bottom left) Hoechst staining in blue. Top right) Histone H3 phosphorylated on S10 in red Bottom right) Overlay with scale: 20 µm. **B**. The percent dividing cells was determined by counting with Image J software on three fields from two slides corresponding to two independent transfections with dsRNA, three days after transfection

(Lampson and Grishchuk 2017)), chromosome segregation defects can occur and are associated with severe developmental abnormalities and diseases, including cancer. We hypothesized that such errors would be more frequent in cultured cells depleted of kinetochore proteins by RNAi, and that this might account for the increase in mitotic index observed following the depletion of CENP-L or NDC80. We used a combination of DNA and tubulin staining to identify defects of spindle structure or of the alignment of the chromosomes on the metaphase plate according to a published description and classification of defects (Baudoin and Cimini 2018; Maiato et al. 2003). Unlike the control (Fig. 4, A), cells depleted of NDC80 contained unaligned chromosomes and multipolar metaphase plates (Fig. 4, B) and metaphase plates of cells depleted of CENP-L contained unaligned chromosomes (Fig. 4, C). No abnormalities were detected in cells depleted of CENP-S or CENP-X (not shown). We were able to quantify the defects observed despite the low proportion of dividing cells and our inability to synchronize the cell culture, through a careful analysis of metaphase plates and mitotic spindles from 60–80 dividing cells from two independent transfections with dsRNA. The number of cells with unaligned chromosomes was 2.4 times higher and that of cells with abnormal mitotic spindles was 2.7 times higher after transfection with a dsRNA against *cenp*-L than after transfection with a dsRNA against *gfp;* the corresponding numbers were 4.7 and 5.5 higher, respectively, following transfection with a dsRNA against *ndc*80 than after transfection with a dsRNA against *gfp* (Fig. 4, D).

Attempts to visualize the centromere during cell division

To visualize the centromere during cell division, we constructed fusion proteins of CENP-L, -S and –X with green fluorescent protein, GFP, using the set of Gateway-compatible vectors for live imaging in insect cells developed by (Maroniche et al. 2011). We amplified the genes of interest by PCR using as template cDNA of the larvae according to Material and methods. The recombinant final plasmids were transfected into *Sf*9 cells in parallel with a control plasmid carrying *Homo sapiens* Lamin B fused to CFP, marker of the nucleus sub-localization (Maroniche et al. 2011) and cells were observed under the microscope 48 h and 72 h post-transfection. We could show that the three proteins fusion CENP-L, -S and –X are located in the nuclei of *Sf*9 cells (Supplementary Fig. 4) in interphase nuclei. However, unfortunately, we could not find figures of metaphase or anaphase, which are usually present in 4–5% of the cells (mitotic indices, Fig. 3), suggesting that overexpression of GFP-tagged proteins impeedes kinetochore formation. We also raised antibodies against peptides chosen within CENP-L and –S sequences, however their specifity was not sufficient to visualize the kinetochore in IF microscopy experiments (not shown).

Discussion

We first studied the patterns of inner and outer kinetochore gene expression *in vivo* in *Spodoptera frugiperda.* We found that these genes were more strongly expressed in the gonadal than in the non-gonadal tissues of the insect. We characterized a subset of these genes in greater detail by developing a protocol for dsRNA-mediated gene silencing in cultured *Spodoptera frugiperda* ovarian cells (Sf9). The depletion of CENP-L or NDC80 led to increases in both mitotic index and the numbers of cells containing unaligned chromosomes or multipolar spindles during metaphase, consistent with a role for these proteins in chromosome segregation.

We used RNA-Seq to compare the expression of kinetochore genes between a tissue with high rates of division (the testis (Salama et al. 1971)) and a tissue with only moderate rates of division (the fat body). In *Bombyx mori*, the testes of fifth-instar larvae are composed of four testicular lobes containing germline stem cells in mitosis at the periphery and spermatocytes at all stages of meiosis up to mature sperm (Rosin et al. 2021). A dissection of *S. frugiperda* larvae revealed a similar organ structure and microscopic analyses of chromosome spreads showed chromosomes undergoing mitosis, which appeared tiny, and chromosomes in the prophase of meiosis, which appeared elongated (Supplementary Fig. 1) as was shown in a close species (Salama et al. 1971). Transcriptomic analysis showed that 16 of the 17 (94%) known kinetochore genes were more strongly expressed in the testis than in the fat body, a somatic tissue with moderate levels of mitotic activity (Skowronek et al. 2021). All the known kinetochore genes of *S. frugiperda* had similar patterns of expression, as expected for genes involved in the same biological process, except for *cenp-S,* which was expressed at similar low levels in both tissues. The homolog of *cenp-B* that we characterized in a previous study (d'Alencon et al. 2011) was also more strongly expressed in the gonads than in the fat body (Supplementary Table 1, tab DESeq2). We were unable to identify any previous publications on kinetochore gene expression in *Bombyx mori*, but the CENP-T protein has been shown to be present in the kinetochore during meiosis I in the larval testis (Rosin et al. 2021). Our transcriptomic results suggest that most kinetochore proteins are present during both mitosis and meiosis, even though the mitotic and meiotic kinetochore assembly pathways differ in Lepidoptera and may involve different components (Melters et al. 2012; Rosin et al. 2021).

The silencing of CENP-L or NDC80 in *Sf*9 cells resulted in a larger number of cells with chromosome segregation defects than observed in control cells (Figs. 4, D). Similar

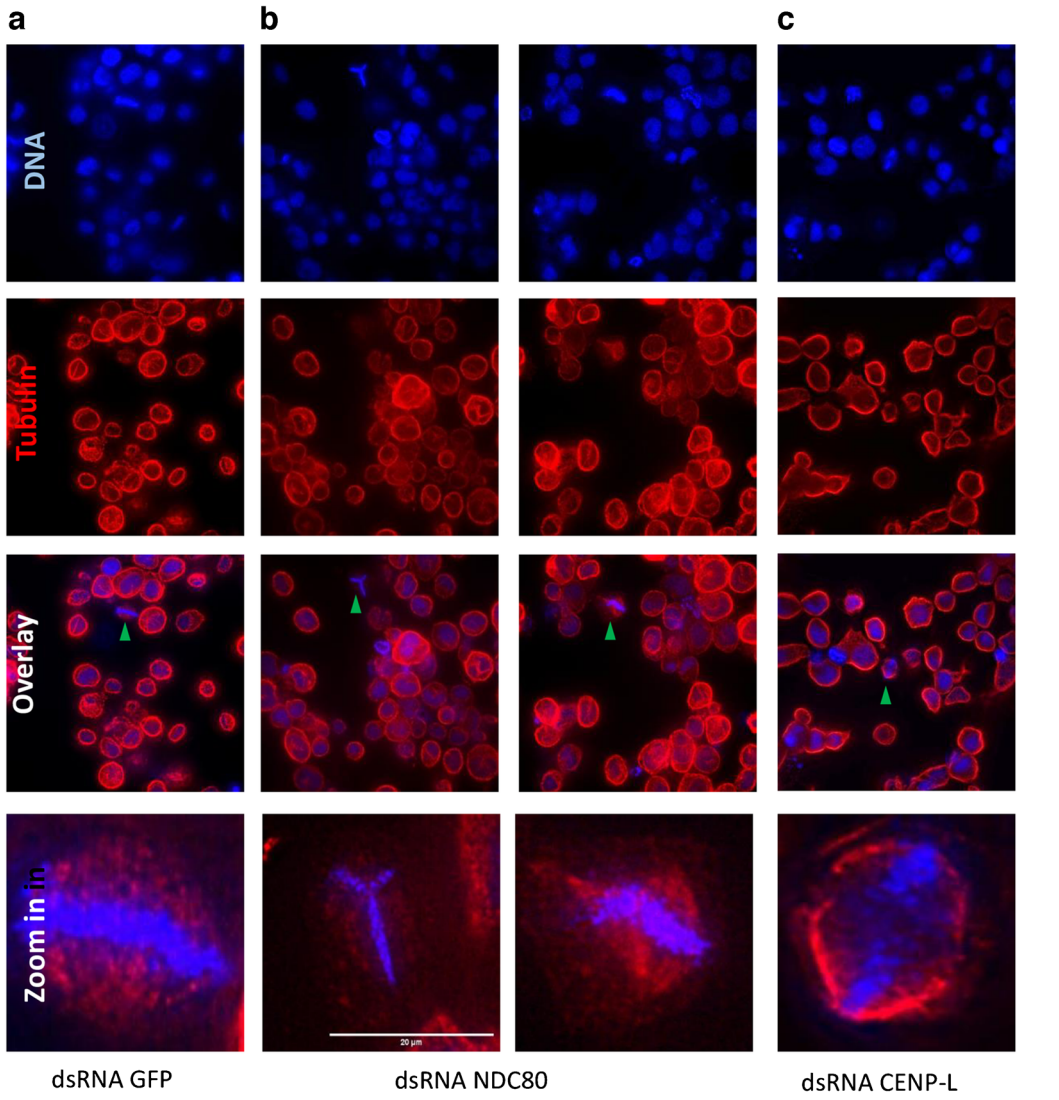
a
b
c
DNA
Tubulin
Overlay
Zoom in in
dsRNA GFP
dsRNA NDC80
dsRNA CENP-L

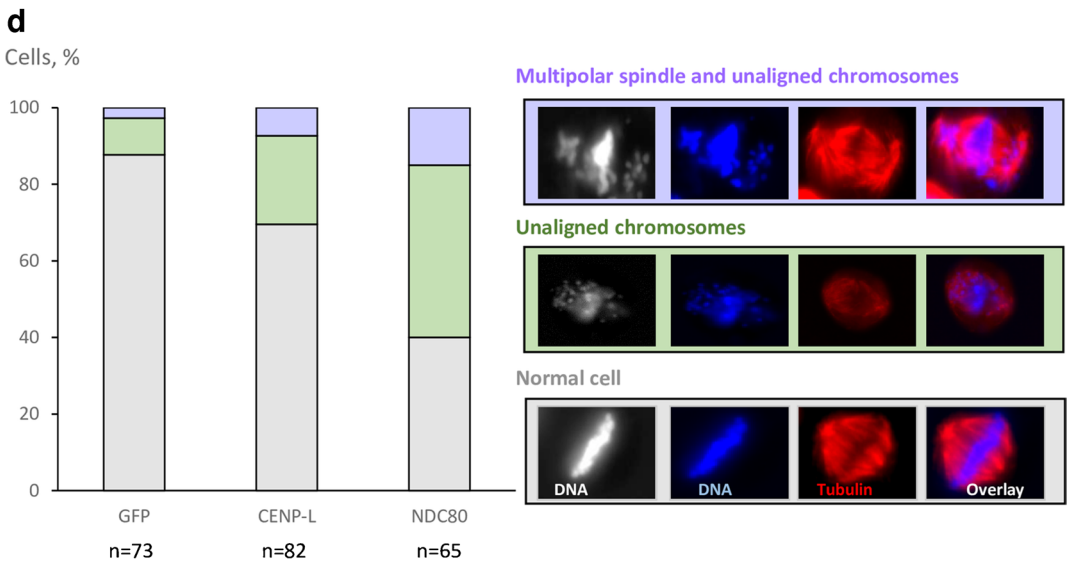
d
Cells, %
100
80
60
40
20
0
GFP
CENP-L
NDC80
n=73
n=82
n=65
Multipolar spindle and unaligned chromosomes
Unaligned chromosomes
Normal cell
DNA
DNA
Tubulin
Overlay

◂**Fig. 4** Representative images of cell division defects observed by microscopy, and their quantification after kinetochore protein depletion. The images shown correspond to a single z-plane. From top to bottom: Hoechst staining in blue; tubulin staining in red, Overlay, zoom on a control cell or the defect observed. The magnified cells are indicated by a green triangle on the overlay. **a**) Normal division in cells transfected with the dsRNA against *gfp*. **b**) Depletion of NDC80. **c**) Depletion of CENP-L. **d**) Histograms showing the percentages of cells showing no defect (gray), with unaligned chromosomes (yellow), and with a combination of unaligned chromosomes and mitotic spindle defects after transfection with the dsRNAs against *gfp* (control), *cenp*-L and *Ndc*80. DNA on grayscale or in blue, spindles in red and overlay

phenotypes have been reported in vertebrate cells: the inducible CRISPR-Cas9 based knockout of CENP-L or CENP-N, with which CENP-L interacts, leads to chromosome misalignment in human cell culture (McKinley et al. 2015; Navarro and Cheeseman 2022). Microinjections of antibodies against HEC1 (NDC80) into cultured human cells lead to the disorganization of mitotic spindles with, in many cases, multiple spindle poles observed (Chen et al. 1997).

Similarly, in the lepidopteran model *Bombyx mori*, Mon et al. (2017) characterized outer kinetochore proteins and showed by flow cytometry that NDC80 depletion induced cell cycle arrest in Bm N4-SID1 cells (Mon et al. 2017). Coste-Silva used dsRNA to deplete Bm N4 cells of certain CCAN genes (encoding CENP-N, CENP-M, CENP-I, CENP-T) and outer kinetochore genes (Spc24, Dsn1). They also observed unaligned chromosomes and congression defects for knockouts of the outer kinetochore genes and milder phenotypes for the depletion of CCAN components, as in our study (Cortes-Silva et al. 2020).

In our study, the silencing of CENP-L and NDC80 modified mitotic index, whereas the silencing of CENP-S and X did not. The phenotype is different in vertebrates. Chicken DT40 cells with mutations of CENP-S and CENP-X are viable but their cell cycle progression is abnormal, and HeLa cells transfected with a siRNA against CENP-X have unaligned metaphase chromosomes (Amano et al. 2009), demonstrating the importance of these proteins for stable kinetochore assembly. However, Mon et al. reported that the depletion of CENP-S or CENP-X in *Bombyx mori* cells did not induce cell cycle arrest, as demonstrated by flow cytometry (Mon et al. 2017). Our findings are also consistent with the lack of detection of these two proteins in previous IP-MS analyses targeting known kinetochore components in *S. frugiperda* cells (Cortes-Silva et al. 2020). Together, these findings suggest that the CENP-S and CENP-X proteins are not critical components for the recruitment of the outer kinetochore assembly in Lepidoptera, unlike CENP-T, which has been shown to play a key role in this process (Cortes-Silva et al. 2020). We raised antibodies against selected peptides from the CENP-S protein sequence (as well as CENP-L). Unfortunately, inconclusive results were obtained when these antibodies were used to check the depletion of the protein by IF analysis (not shown). In this study, we also constructed fusion proteins of CENP-L, -S, -X with GFP and could show by live imaging that the three proteins are located in the nucleus of *Sf*9 cells (Supplementary Fig. 4). Unfortunately, we could not observe their localization during cell division. Because the transfection efficiency is less than 10% and because we expect less than 5% of cells dividing, we have a chance to observe division in 0.5% of the cells, which is low. The overexpression of the fusion proteins may impede kinetochore assembly contributing to a much lower rate. Efforts are still needed in future to localize the proteins under study during M phase to definitively show that *Sf* CENP-L and NDC80 play a role during chromosome segregation and to check if the two other proteins CENP-S and -X are indeed associated to the kinetochore.

Our protocol for RNAi-mediated silencing in *Sf*9 cells made it possible to assess kinetochore gene function at a small scale *in vitro*. This approach could easily be transposed to other gene sets. However, our study was limited by the asynchronous growth of the cell population, with no more than 4% of the cells dividing at any given time; the analysis of a large number of cells was therefore required to detect mitotic division defects (Cortes-Silva et al. 2020). Further efforts are required to achieve cell synchronization and to overcome other problems encountered in the use of RNAi in lepidopterans *in vivo*.

We describe here the first study of the pattern of CENP-L expression and of the effects of depleting this protein in Lepidoptera. Based on a recent analysis of the structure of the CCAN in the model proposed by Pesenti et al., this protein and its paralog CENP-N play a crucial role in the formation of a vault between two pillars composed of other CCAN components with a base consisting of CENP-T and CENP-W (Pesenti et al. 2022; Yatskevich et al. 2022). This vault is thought to accommodate a linker DNA between CENP-A nucleosomes but it cannot accommodate centromeric nucleosomes themselves; these centromeric nucleosomes, thus, remain outside of this structure, with CENP-C linking the CENP-A in centromeric nucleosomes to CENP-N (Pesenti et al. 2022; Yatskevich et al. 2022). We hypothesize that this vault structure — including CENP-L, CENP-N, the pillars and the base — is conserved in the holocentric chromosomes of insects lacking CENP-C and CENP-A, with the CENP-A nucleosomes either simply absent or replaced by nucleosomes carrying histone H3 trimethylated on lysine 27 (H3K27me 3), which has been shown to be positively associated with CENP-T in *Bombyx mori* cell culture (Senaratne et al. 2021). However, this association is not perfect, as CENP-T also localizes to K27me3-negative regions. K27me3 cannot therefore be considered to act as a marker for kinetochore recruitment. Additional functional studies are required *in vivo* and *in vitro* to obtain a clearer picture

of the assembly of kinetochores on the holocentromere in concert with chromatin dynamics.

Conclusion

We report here the successful silencing of kinetochore genes in *Spodoptera frugiperda* cells and provide evidence for the involvement of CENP-L and NDC80 homologs in the segregation of holocentric chromosome, with CENP-S and CENP-X playing a minor role. This study provides the first clues to the role of CENP-L in Lepidoptera and constitutes a necessary step towards identifying the location of the corresponding gene target in the *S. frugiperda* genome by chromatin immunoprecipitation.

Supplementary Information The online version contains supplementary material available at https://doi.org/10.1007/s00412-025-00828-2.

Acknowledgements We thank Vicky Diakou and Elodie Jublanc for their assistance with microscopy at the BIOCAMPUS MRI-DBS OPTIQUE platform at the University of Montpellier. We thank Philippe Clair of the BIOCAMPUS qPHD platform at the University of Montpellier for his help with qPCR analysis. This work was supported by two grants from the Plant Health and Environment Division of INRAE: a "HOLOCEN" grant awarded to Emmanuelle d'Alençon and a "CENTROVIR" grant awarded to Isabelle Darboux.

Authors' contributions Conception and design: E.A. Acquisition of data, analysis and interpretation: S.Ga, S.Gi, M.E., F.L. and E.A. Drafting and revision of the manuscript: S. Ga., S.Gi., F.L. and E.A.

Funding This work was supported by grants from the Plant Health and Environment Division of INRAE.

Availability of data and materials RNA-Seq from gonads are available at NCBI under accession number SAMN40291315.

Declarations

Ethical approval The authors state that experimental research presented here complies with the relevant institutional guidelines and legislation.

Consent to participate Not applicable.

Consent for publication All the authors have given a consent for publication.

Competing interests The authors declare no competing interests.

References

Agrawal N, Malhotra P, Bhatnagar RK (2004) siRNA-directed silencing of transgene expressed in cultured insect cells. Biochem Biophys Res Commun 320:428–434

Amano M, Suzuki A, Hori T, Backer C, Okawa K, Cheeseman IM, Fukagawa T (2009) The CENP-S complex is essential for the stable assembly of outer kinetochore structure. J Cell Biol 186:173–182

Anders S, Huber W (2010) Differential expression analysis for sequence count data. Genome Biol 11:R106

Baudoin NC, Cimini D (2018) A guide to classifying mitotic stages and mitotic defects in fixed cells. Chromosoma 127:215–227

Bossin H, Fournier P, Royer C, Barry P, Cérutti P, Gimenez S, Couble P, Bergoin M (2003) JcDNV-based vectors for stable transgene expression in Sf9 cells: influence of the densovirus sequences on genomic integration. J Virol. 77:11060–11071

Buchwitz BJ, Ahmad K, Moore LL, Roth MB, Henikoff S (1999) A histone-H3-like protein in C. elegans. Nature. 401:547–548

Chen YM, Riley DJ, Chen PL, Lee WH (1997) HEC, a novel nuclear protein rich in leucine heptad repeats specifically involved in mitosis. Mol Cell Biol 17:6049–6056

Chen X, Koo J, Gurusamy D, Mogilicherla K, Reddy Palli S (2021) Caenorhabditis elegans systemic RNA interference defective protein 1 enhances RNAi efficiency in a lepidopteran insect, the fall armyworm, in a tissue-specific manner. RNA Biol 18:1291–1299

Coghlan A, Wolfe KH (2002) Fourfold faster rate of genome rearrangement in nematodes than in Drosophila. Genome Res 12:857–867

Cortes-Silva N, Ulmer J, Kiuchi T, Hsieh E, Cornilleau G, Ladid I, Dingli F, Loew D, Katsuma S, Drinnenberg IA (2020) CenH3-Independent Kinetochore Assembly in Lepidoptera Requires CCAN, Including CENP-T. Curr Biol 30:561-572.e10

d'Alencon E, Sezutsu H, Legeai F, Permal E, Bernard-Samain S, Gimenez S, Gagneur C, Cousserans F, Shimomura M, Brun-Barale A et al (2010) Extensive synteny conservation of holocentric chromosomes in Lepidoptera despite high rates of local genome rearrangements. Proc Natl Acad Sci U S A 107:7680–7685

d'Alencon E, Negre N, Stanojcic S, Alassoeur B, Gimenez S, Leger A, Abd-Alla A, Juliant S, Fournier P (2011) Characterization of a CENP-B homolog in the holocentric Lepidoptera Spodoptera frugiperda. Gene 485:91–101

Dumont J, Oegema K, Desai A (2010) A kinetochore-independent mechanism drives anaphase chromosome separation during acentrosomal meiosis. Nat Cell Biol 12:894–901

Gerbal M, Fournier P, Barry P, Mariller M, Odier F, Devauchelle G, Duonor-Cerutti M (2000) Adaptation of an insect cell line of Spodoptera frugiperda to grow at 37 degrees C: characterization of an endodiploid clone. In Vitro Cell Dev Biol Anim 36:117–124

Gouin A, Bretaudeau A, Nam K, Gimenez S, Aury JM, Duvic B, Hilliou F, Durand N, Montagne N, Darboux I et al (2017) Two genomes of highly polyphagous lepidopteran pests (Spodoptera frugiperda, Noctuidae) with different host-plant ranges. Sci Rep 7:11816

Gurusamy D, Mogilicherla K, Shukla JN, Palli SR (2020) Lipids help double-stranded RNA in endosomal escape and improve RNA

interference in the fall armyworm. Spodoptera Frugiperda Arch Insect Biochem Physiol 104:e21678
Hendzel MJ, Wei Y, Mancini MA, Van Hooser A, Ranalli T, Brinkley BR, Bazett-Jones DP, Allis CD (1997) Mitosis-specific phosphorylation of histone H3 initiates primarily within pericentromeric heterochromatin during G2 and spreads in an ordered fashion coincident with mitotic chromosome condensation. Chromosoma 106:348–360
Hockens C, Lorenzi H, Wang TT, Lei EP, Rosin LF (2024) Chromosome segregation during spermatogenesis occurs through a unique center-kinetic mechanism in holocentric moth species. PLoS Genet 20:e1011329
Holm PB, Rasmussen SW (1980) Chromosome-Pairing, Recombination Nodules and Chiasma Formation in Diploid Bombyx Males. Carlsberg Res Commun 45:483–548
Howe M, McDonald KL, Albertson DG, Meyer BJ (2001) HIM-10 is required for kinetochore structure and function on Caenorhabditis elegans holocentric chromosomes. J Cell Biol 153:1227–1238
Ishii M, Akiyoshi B (2022) Plasticity in centromere organization and kinetochore composition: Lessons from diversity. Curr Opin Cell Biol 74:47–54
Jacobsen LB, Calvin SA, Colvin KE, Wright M (2004) FuGENE 6 Transfection Reagent: the gentle power. Methods 33:104–112
Lampson MA, Grishchuk EL (2017) Mechanisms to avoid and correct Erroneous Kinetochore-Microtubule attachments. Biology (Basel) 6:1
Li Y, Jousset FX, Giraud C, Rolling F, Quiot JM, Bergoin M (1996) A titration procedure of the Junonia coenia densovirus and quantitation of transfection by its cloned genomic DNA in four lepidopteran cell lines. J Virol Methods 57:47–60
Lukhtanov VA, Dinca V, Friberg M, Sichova J, Olofsson M, Vila R, Marec F, Wiklund C (2018) Versatility of multivalent orientation, inverted meiosis, and rescued fitness in holocentric chromosomal hybrids. Proc Natl Acad Sci USA 115:E9610–E9619
Maiato H, Sunkel CE, Earnshaw WC (2003) Dissecting mitosis by RNAi in Drosophila tissue culture cells. Biological Procedures Online 5:153–161
Mandrioli M, Manicardi GC (2020) Holocentric chromosomes. Plos Genet. 16:e1008918
Maroniche GA, Mongelli VC, Alfonso V, Llauger G, Taboga O, del Vas M (2011) Development of a novel set of Gateway-compatible vectors for live imaging in insect cells. Insect Mol Biol 20:675–685
McAinsh AD, Kops G (2023) Principles and dynamics of spindle assembly checkpoint signalling. Nat Rev Mol Cell Biol 24:543–559
McKinley KL, Sekulic N, Guo LY, Tsinman T, Black BE, Cheeseman IM (2015) The CENP-L-N Complex Forms a Critical Node in an Integrated Meshwork of Interactions at the Centromere-Kinetochore Interface. Mol Cell 60:886–898
Melters DP, Paliulis LV, Korf IF, Chan SW (2012) Holocentric chromosomes: convergent evolution, meiotic adaptations, and genomic analysis. Chromosome Res 20:579–593
Mon H, Lee JM, Sato M, Kusakabe T (2017) Identification and functional analysis of outer kinetochore genes in the holocentric insect Bombyx mori. Insect Biochem Mol Biol 86:1–8
Mon H, Sato M, Lee JM, Kusakabe T (2022) Construction of gene co-expression networks in cultured silkworm cells and identification of previously uncharacterized lepidopteran-specific genes required for chromosome dynamics. Insect Biochem Mol Biol 151:103875
Monen J, Maddox PS, Hyndman F, Oegema K, Desai A (2005) Differential role of CENP-A in the segregation of holocentric C. elegans chromosomes during meiosis and mitosis. Nat Cell Biol 7:1248–1255
Nam K, Nhim S, Robin S, Bretaudeau A, Nègre N, d'Alençon E (2018) Divergent selection causes whole genome differentiation without physical linkage among the targets in Spodoptera frugiperda (Noctuidae). bioRxiv. https://doi.org/10.1101/452870
Navarro AP, Cheeseman IM (2022) Dynamic cell cycle-dependent phosphorylation modulates CENP-L-CENP-N centromere recruitment. Mol Biol Cell 33:er87
Pesenti ME, Raisch T, Conti D, Walstein K, Hoffmann I, Vogt D, Prumbaum D, Vetter IR, Raunser S, Musacchio A (2022) Structure of the human inner kinetochore CCAN complex and its significance for human centromere organization. Mol Cell 82:2113–2131
Poitout S, Bues R (1974) Linolenic acid requirements of lepidoptera Noctuidae Quadrifinae Plusiinae: Chrysodeixis chalcites Esp., Autographa gamma L'. Macdunnoughia confusa Stph., Trichoplusia ni Hbn. reared on artificial diets. Ann Nutr Aliment 28:173–187
Prigent C, Dimitrov S (2003) Phosphorylation of serine 10 in histone H3, what for? J Cell Sci 116:3677–3685
Robin S, Legeai F, Jouan V, Ogliastro M, Darboux I (2023) Genome-wide identification of lncRNAs associated with viral infection in Spodoptera frugiperda. J Gen Virol 104:001827
Rosin LF, Gil J, Drinnenberg IA, Lei ELP (2021) Oligopaint DNA FISH reveals telomere-based meiotic pairing dynamics in the silkworm, Bombyx mori. Plos Genet 17:e1009700
Salama A, Abdellatif MA, Bakry NMS (1971) Developmental Differentiation of the Reproductive System in the Cotton Leaf Worm Spodoptera littoralis (Bois.). Zeitschrift für Angewandte Entomologie 68:308–314
Senaratne AP, Muller H, Fryer KA, Kawamoto M, Katsuma S, Drinnenberg IA (2021) Formation of the CenH3-Deficient Holocentromere in Lepidoptera Avoids Active Chromatin. Curr Biol 31:173-181.e7
Skowronek P, Wójcik L, Strachecka A (2021) Fat Body-multifunctional insect tissue. Insects 12:547
Somma MP, Ceprani F, Bucciarelli E, Naim V, De Arcangelis V, Piergentili R, Palena A, Ciapponi L, Giansanti MG, Pellacani C et al (2008) Identification of Drosophila mitotic genes by combining co-expression analysis and RNA interference. PLoS Genet 4:e1000126
Westhorpe FG, Straight AF (2013) Functions of the centromere and kinetochore in chromosome segregation. Curr Opin Cell Biol 25:334–340
Xu J, Nagata Y, Mon H, Li Z, Zhu L, Iiyama K, Kusakabe T, Lee JM (2013) Soaking RNAi-mediated modification of Sf9 cells for baculovirus expression system by ectopic expression of Caenorhabditis elegans SID-1. Appl Microbiol Biotechnol 97:5921–5931
Yatskevich S, Muir KW, Bellini D, Zhang ZG, Yang J, Tischer T, Predin M, Dendooven T, McLaughlin SH, Barford D (2022) Structure of the human inner kinetochore bound to a centromeric CENP-A nucleosome. Science 376:844–852
Zedek F, Bures P (2018) Holocentric chromosomes: from tolerance to fragmentation to colonization of the land. Ann Bot 121:9–16